Coherent theta-band EEG activity predicts item-context binding during encoding

Christopher Summerfield* and Jennifer A. Mangels

Psychology Department, Columbia University, New York, NY 10027, USA

Episodic memories consist of semantic information coupled with a rich array of contextual detail. Here, we investigate the neural processes by which information about the sensory context of a learning event is "bound" to the semantic representation of the to-be-encoded item. We present evidence that item-context binding during encoding is mediated by frontoposterior electroencephalographic (EEG) phase locking within and between hemispheres in the theta (4–8 Hz) band. During a task in which subjects encoded words in different font colors, later memory for the word was associated with sustained frontal theta activity and frontoposterior theta-band coherence, primarily within the left hemisphere. When the word-color association was later successfully retrieved, however, neurons synchronized their theta-band responses bilaterally in a more sustained fashion, particularly during the latter part of the stimulus epoch (>800 ms). Our results confirm the importance of functional coupling between frontal and posterior regions for successful encoding. One interpretation of these data is hemispheric contributions to item and context encoding may be asymmetric, with left hemisphere coherence facilitating semantic processing of an item and right hemisphere coherence facilitating processing of sensory context. Theta-band coherence may be an important mechanism by which brain networks exchange information during learning.
© 2004 Elsevier Inc. All rights reserved.

Keywords: Memory; Encoding; Episodic; Source; Context; Electroencephalography (EEG); Theta; Coherence; Binding; Independent components analysis (ICA)

Introduction

Learning new information about the world requires dynamic collaboration between multiple brain structures. Observations from patient and brain imaging studies have converged to suggest that the process by which information is encoded into long-term memory relies upon diverse areas of the frontal and parietal lobes (Janowsky et al., 1989; Otten et al., 2002; Wagner et al., 1998), as well as the medial temporal lobe structures implicated by initial lesion studies (Scoville and Milner, 1957). However, while there is good agreement about the functional neuroanatomical correlates of encoding, so far few studies have addressed how different brain regions may interact during the formation of new memories.

Recent 'dynamicist' approaches to brain function, which emphasize the importance of understanding the neural signal by which spatially separate brain areas interact during cognition, have looked to phase synchronization of neural oscillations as a candidate code by which information is shared between spatially separate brain regions (Engel et al., 2001). In support of this contention, studies in diverse areas of cognition, including perception (Rodriguez et al., 1999), sensorimotor integration (Roelfsema et al., 1997), and working memory (Sarnthein et al., 1998), have reported greater electroencephalographic (EEG) phase locking (or 'coherence') across the brain for tasks that demand greater integration of information. These reports have led some researchers to conjecture that EEG coherence reflects the fundamental mechanism by which the brain "functionally couples" information across neural space for the purpose of perceptual or attentional binding, sensory awareness, and even our subjective sense of self (Crick and Koch, 1990; Jensen and Lisman, 1996; Singer and Gray, 1995; Tononi and Edelman, 1998; Varela, 1995).

Preliminary evidence suggests that neural synchronization may also play a role in successful encoding into long-term memory. Neurophysiological studies in lower mammals have suggested that encoding may be supported by local or long-range synchronization of hippocampal or neocortical theta-band (4–8 Hz) EEG activity. For example, long-term potentiation, the candidate cellular–molecular basis for the formation of new memories, appears to depend on the phase of hippocampal theta activity (Huerta and Lisman, 1993), and blocking theta activity by lesioning the medial septum causes spatial memory impairments (Givens and Olton, 1990). In addition, recent data from intracranial EEG studies in patients with medial temporal lobe epilepsy have shown that functional coupling in the theta-band

* Corresponding author. Psychology Department, Schermerhorn Hall, Room 406, Columbia University, 1190 Amsterdam Avenue, New York, NY 10027, USA.
E-mail address: summerfd@psych.columbia.edu (C. Summerfield).
Available online on ScienceDirect (www.sciencedirect.com).

between hippocampal and rhinal cortices is correlated with successful encoding (Fell et al., 2003).

Theta-band activity at the cortical level also appears to have a role in creating long-term memories. Scalp EEG recordings in humans have shown that local increases in theta activity over medial frontal electrode sites accompany successful encoding (Klimesch et al., 1996), and intracranial EEG recordings have confirmed that frontal and right temporal neocortical sites exhibit local increases in synchrony during successful encoding (Sederberg et al., 2003). In addition, two studies thus far have reported increases in long-range coherent activity between frontal and temporo-parietal regions during the encoding of words that were later successfully retrieved (Sauseng et al., 2004; Weiss and Rappelsberger, 2000). Nonetheless, whether theta-band activity mediates functional coupling between cortex and hippocampus during learning remains to be demonstrated (Buzsaki, 1996; Kahana et al., 1999).

In previous EEG studies of encoding-related theta activity, the criterion for successful encoding was later word recognition or recall (Klimesch et al., 1996; Sauseng et al., 2004; Sederberg et al., 2003; Weiss and Rappelsberger, 2000). Yet, information about the world is rarely encoded in isolation. Our memories are composed of semantic information coupled with a rich array of associated contextual detail, which may include the place or time the information was encoded, ongoing mentation that accompanies the encoding episode, or featural details about the stimulus. Recent neuroimaging and ERP studies have begun to explore how the neural mechanisms that are active during the encoding of an item alone ('item' encoding) may differ from those subserving encoding of an item and associated contextual information ('item + context' encoding) (Cansino et al., 2002; Davachi et al., 2003; Duarte et al., 2004; Ranganath et al., 2004). Although many studies have focused primarily on how medial temporal lobe structures differ with respect to encoding of item and context, several have also reported that both frontal and posterior neocortical sites tend to be differentially active on encoding trials that lead to later successful memory for the item + context association, as compared to trials were the item is correctly recognized, but the context is not. For example, Cansino et al. (2002) report increased activity in the left prefrontal regions and the right lateral occipital complex that predicts later memory for a picture in a given spatial location when compared to brain activity predictive of later recognition of the picture alone. In another study employing a task involving memory for word-color associations, items eliciting correct word-color recognition at test exhibited greater activation at encoding in bilateral cortical regions including inferior prefrontal brain areas, as well as right fusiform regions proximal to the parahippocampal gyrus, than items that were correctly recognized but associated with the incorrect color (Ranganath et al., 2004). One hypothesis that arises from these data is that 'binding' of item and context during encoding requires the exchange of information between frontal and posterior brain regions bilaterally. Previous reports of frontoposterior coherence during encoding and working memory provide additional support for this proposal (Sarnthein et al., 1998; Sauseng et al., 2004; Weiss and Rappelsberger, 2000). Given that EEG permits an examination not just which brain regions may be active under given task conditions, but whether these regions are 'functionally coupling' in a dynamic network, we set out to determine whether patterns of frontoposterior theta-band coherence, both within each hemisphere and between the two hemispheres, dissociate item encoding from item + context encoding.

We recorded ongoing EEG while subjects encoded words presented in one of four different font colors. Although there are many possible types of 'context' that may be encoded alongside an item, color represents a type of intrinsic, sensory context. In addition, stimuli of a similar type were employed by one of the recent studies showing frontal and posterior contributions to encoding (Ranganath et al., 2004). This task allowed us to classify encoding trials on the basis of three levels of later memory performance: trials on which the word + color association was successfully encoded (WC trials), trials on which successful word recognition occurred but without encoding of the associated color (WO trials), and trials on which word recognition later failed (Miss trials). Using post hoc comparisons between conditions (WC > Miss, WO > Miss, and WC > WO), we were thus able to dissociate effects that were specific to successful item encoding (results significant for comparisons WC > Miss and WO > Miss) from effects specific to item + context encoding (results significant for WC > Miss and WC > WO).

Finally, we present a novel method to deal with the large quantity of data that has to be processed and statistically compared when analyzing EEG coherence. Increasingly, independent components analysis (ICA) is being used to reduce data in fMRI and ERP studies to a tractable set of spatially independent components (McKeown et al., 2003). ICA provides a "blind" solution to the separation of linearly mixed, statistically independent inputs, without the constraint of orthogonalizing the factors inherent to PCA (Bell and Sejnowski, 1995). Therefore, in addition to conventional comparisons at each electrode, we present a method for the analysis of time–frequency (TF) and coherence data that uses ICA to reduce the data to spatially correlated patterns of activity.

Materials and methods

Subjects

Nineteen paid volunteers (14 women) were recruited via posters placed in Columbia University psychology department. Subjects were neurologically normal right-handers aged between 19 and 38 years old. All subjects gave informed consent to participate in the study, which was approved by Columbia University Institutional Review Board.

Procedure

Four study-test blocks were presented. In the study/encoding phase, subjects viewed lists of 45 successively presented medium-frequency (length 3–11 letters) nouns in one of four font colors: red, yellow, green, or blue. Words remained on the screen for 2000 ms and were followed by a blank screen for 1000 ms. Subjects were instructed to remember as many of the 45 word-color associations as possible. Following a brief distracter task (counting backwards by threes from a random three-digit number for 20 s), subjects undertook the test/retrieval phase, in which they were presented with 90 probe words in white font, half of which were old (i.e., had been shown in the immediately prior encoding phase) and half of which were new (distracters). Following presentation of the word (2000 ms), subjects were prompted to make a key press to indicate whether the probe was old or new, and to assess their confidence in this judgment, by responding in one of four categories: "sure old", "think old", "think new", or "sure new". Immediately following this response, a second prompt appeared, asking subjects to indicate in which of the four font colors the word had been presented. Again, for

each option, subjects could indicate that they were "sure" or that they "guessed" that this was correct, giving a total of eight response options ("sure red", "guess red", "sure blue", etc). Following this response, a blank screen was presented for 1000 ms, and then the next memory probe.

EEG recording and artifact rejection

EEG activity was recorded during the encoding and retrieval phases of the experiment, although in this report, only data from the encoding phase are discussed. EEG was acquired from 64 channels (sampling rate = 500 Hz; high pass filter = 0.1 Hz, low pass filter = 100 Hz; impedances kept below 11 kΩ) using Neuroscan SYNAMPS (Compumedics Inc., El Paso, TX). Recordings were initially referenced to Cz, then converted to an average reference off-line. BESA 5.06 (Electrical Geodesics Inc., Eugene, OR) was used to remove eye movements, blinks, and other artifacts from the continuous EEG data (Berg and Scherg, 1994). Trials in which muscle, movement, or other artifacts drove amplitude values above 100 μV were manually rejected. Artifact-free data were high-pass filtered with a 0.5-Hz zero-phase filter, spline-laplacian transformed (estimated dura potential (Nunez et al., 1997), and interpolated into an 81-electrode montage. Epochs from 1000 ms prestimulus to 2000 ms poststimulus were then exported into ASCII format.

Data analysis with BEAST

All further data processing was performed with in-house MATLAB software written by the authors. The code used for signal processing and analysis (BEAST—Brain Electrophysiology Analysis and Statistical Testing) may be freely downloaded at www.columbia.edu/~cs2028/beast/beast.htm. Under the framework of this analysis package, data processing consists of various stages: (1) signal preprocessing, (2) conventional time–frequency and coherence analyses at each electrode or electrode pairing (here referred to as 'electrode-wise' or 'pairing-wise' analyses, or collectively as 'e/p-wise analyses'), (3) spatial ICA on time–frequency and coherence data. The logic of using ICA in parallel with conventional between-condition comparisons at each electrode site arises from the intersecting problems of data visualization and correction for multiple comparisons in significance testing that are central to the reporting of results from neuroimaging studies. Neuroimaging experiments routinely acquire thousands of observations from the brain simultaneously, but a clear approach to determining the statistical independence of the observations, and thus the appropriate way to correct for multiple comparisons, has yet to be agreed upon for EEG data. ICA is used here as a complement to conventional statistical comparisons under the premise that the spatial components derived are statistically independent, and thus corrections for multiple comparison need only account for the number of components (here, 4) rather than the total number of spatial observations (here, 81 for TF analyses; 190 for coherence analyses).

Preprocessing

ASCII files of epoched data were imported into MATLAB. First, data were baseline corrected by subtracting the mean amplitude of the first 500 ms of the epoch (−1000 to −500 ms prestimulus) from the entire epoch. This served to remove nonstationarities (slow

changes in EEG amplitude). We chose not to baseline correct with the period immediately prior to the stimulus in order to permit us to examine prestimulus (−500 to 0 ms) changes in EEG activity that may be predictive of subsequent memory. Many previous EEG studies have measured event-related synchronization (ERS) or desynchronization (ERD) in a given frequency band, in which spectral power is expressed as a percentage change from a prestimulus baseline. This method does not permit dissociation between prestimulus and poststimulus changes in spectral power. However, pilot studies in our lab have shown that in some cases, prestimulus changes in spectral power (for example, in the alpha-band) may be associated with the effects of interest (although no such results are reported in the present article). We thus performed amplitude baselining using an epoch ending 500 ms prior to stimulus presentation. Secondly, the ERP, taken as the mean across all trials, was subtracted from each epoch to remove stimulus-locked activity. This procedure leaves the 'induced' (jittered in time with respect to the stimulus) theta activity. At least in higher frequency bands, it is the induced activity that has been more specifically associated with neural integration or 'binding' (Tallon-Baudry and Bertrand, 1999).

Time–frequency (TF) decomposition

All epochs were Morlet wavelet-transformed (Torrence and Campo, 1998) between 4.3 and 7.8 Hz in nine equally space frequency bands. To reduce artifacts, wavelet values were trimmed at five standard deviations above the mean. Data were temporally smoothed with a Gaussian filter of width 100 ms and averaged across adjacent frequency bands. Trials in each condition were subsequently averaged, yielding mean time–frequency information for each condition, at each electrode, for each subject. Averaged wavelet values were converted to z scores at each subject and electrode prior to ICA analyses and significance testing.

Coherence

Coherence was calculated on the cleaned, baseline-corrected, induced EEG data. Due to computational constraints, magnitude-squared coherence was calculated for a subset of 20/81 electrodes (CB1, CB2, Oz, Pz, PO3, PO4, P7, P8, FPz, T7, T8, FCz, FC3, FC4, F7, F8, AF3, and AF4). These representative electrodes provided full scalp coverage with separation of at least 6 cm between any given electrode pair to reduce the likelihood of measuring local synchronous theta activity. The number of electrode pairings from n electrodes is given by $[n(n-1)]/2$, and thus 20 electrodes yielded 190 electrode parings. Coherence was calculated in 2-Hz bins between 4 and 10 Hz (for comparison, activity in the lower alpha band, 8–10 Hz, is also shown, although all reported results in the text are for the theta band, 4–8 Hz) at each of these pairings according to the following formula:

$$\text{Coh}(f) = \frac{\left| \sum\limits_{i=1}^{N} F_1(f) \cdot F_2^*(f) \right|^2}{\sum\limits_{i=1}^{N} \left| F_1(f) \right|^2 \cdot \sum\limits_{i=1}^{N} \left| F_1(f) \right|^2}$$

f is frequency, N is the number of trails involved in averaging, $F_1(f)$ and $F_2(f)$ are Fourier transforms of EEG signal at two different electrodes, and * denotes complex conjugation.

Calculations were made within a sliding Gaussian Fourier window with a width of 500 ms and overlap of 450 ms in order to

yield coherence time–frequency plots (frequency resolution 2 Hz) for each electrode pairing. Coherence values were also calculated for 100 random permutations of the electrode-trial structure (e.g., electrode 1 trial 17, electrode 2 trial 23; electrode 1 trial 5, electrode 2 trial 12, etc), and the z transformed mean of these "shuffled" values was subtracted from the z transformed coherence value from the "intact" (i.e., unshuffled) trial structure at each point in TF space across electrode pairings. We refer to these coherence scores (i.e., intact-shuffled) as "corrected" coherence. The purpose of this correction procedure was to exclude sources of coherence that might occur irrespective of the electrode-trial structure (for example, coherence due to volume conduction, generalized stimulus-locked effects, or spurious coherence values derived from trial counts <30), leaving only coherence that occurs between two electrodes on a given trial for further statistical analysis (Lachaux et al., 2002).

ICA analyses

Spatial ICA was used to decompose TF and coherence data into spatially correlated components. ICA code was adapted from EEGLAB (Delorme and Makeig, 2004). For TF analyses, the four-dimensional data at each electrode (subject * condition * frequency * time) was reshaped to derive an ICA matrix ([81/190] channels * observations). ICA derives as many components as there are input channels, so PCA preprocessing was used to reduce the data to a manageable number of components ($n = 4$) prior to ICA analyses for both TF and coherence analyses (Lee et al., 1999), and these components were considered for statistical analysis. After components reflecting spatially correlated activity across the scalp had been extracted, the component "activations" (time–frequency values for each subject/condition) were derived by multiplying the ICA weights by the original input data. The spatial projection of each component across the scalp was calculated by taking the pseudoinverse of the weights matrix multiplied by the sphering matrix (Delorme and Makeig, 2004), and plotted onto an interpolated scalpmap to show the spatial distribution of each component. For ICA coherence, we additionally plotted the top 10 electrode pairings as grey lines on top of this map.

Significance testing

Significance testing was performed across time-frequency space, both at each electrode/pairing individually (e/p-wise analyses) and on ICA activation scores for each component. Significance testing was carried out with random permutation testing in the following manner: (a) ANOVAs with planned contrasts were conducted at each time–frequency pixel to determine point estimate statistics for each pixel; (b) subject-condition scores were swapped 1000 times, the ANOVA repeated, and the maximum test statistic from the entire time–frequency plot (and, for ICA analyses, component) was logged for each permutation; (c) point estimate statistics that fell within the 95th percentile ($P < 0.05$) of the distribution of maximum shuffled values were deemed to be significant. The distribution of maximum values was used in order to correct for multiple comparisons. This procedure has been described in detail elsewhere (Burgess and Gruzelier, 1999). For e/p-wise analyses, pixels were matched to the distribution of maximum F values across the TF plot at each electrode, rather than the maximum values across all TF plots across all electrodes. For ICA, the distribution of maximum F values across TF space and across all components was employed, thus correcting for statistically independent spatial observations. Scalpmaps were produced in which the percentage of significant TF pixels at each electrode was rendered onto a three-dimensional brain using code adapted from EEGLAB (Delorme and Makeig, 2004).

Results

Task performance

For recognition memory, d' ranged from 0.3 to 3.5 (mean 2.0 ± 0.9). Overall hit rate varied from 61% to 94% (mean $82 \pm 11\%$). Both the word and the font color were correctly retrieved (WC trials) on between 15% and 90% (mean $57 \pm 21\%$) of trials; word alone (WO trials) was retrieved on between 3% and 57% of trials (mean $26 \pm 13\%$). Misses occurred on between 6% and 39% of trials (mean $17 \pm 11\%$). There was also considerable variation in subjects' confidence in responding. Use of high-confidence responses varied between 1% and 100% (mean $59 \pm 25\%$) for the word recognition judgment and between 6% and 93% (mean $68 \pm 24\%$) for the color judgment. High confidence responses were made on $64 \pm 31\%$ of WC trials and on $56 \pm 25\%$ of WO trials. The proportion of high- to low-confidence responses did not differ significantly between WC and WO trials ($P > 0.1$). Thus, to maximize power, we conducted all subsequent EEG analyses on WC, WO, and missed trials collapsed across high and low confidence. In addition, we chose to exclude two subjects who exhibited extremely poor memory performance (d' values of <1 and source memory judgment of <25% [chance]) from these analyses.

Local theta activity: electrode-wise analyses

Fig. 1a shows the mean spectral power in the theta band between 0 and 1500 ms poststimulus, interpolated across the scalp for each of the three conditions. Fig. 1b shows frontal scalp locations at which significant differences were observed for the comparisons WC > Miss (left), WO > Miss (middle), and WC > WO (right). The five electrodes showing the greatest significance for each comparison are labeled on the headmap. No electrodes showed local theta activity that was greater for Miss than for WC or WO trials.

Differences between WC and Miss trials were mainly observed at frontal electrodes bilaterally (Fig. 1b, left panel), with a cluster of left frontal electrodes also showing differences between WO and Miss conditions (Fig. 1b, middle panel). Some electrode sites, such as right frontal electrodes F4, F8, and FC2, also showed differences between WC and WO trials (Fig. 1b, right panel). The time course of theta-band activity for four representative left and right frontal electrodes (F7, AF3, F8, AF4) is shown in Fig. 1c. The positions of these electrodes on the scalp are marked in Fig. 1a. Mean spectral power (in z scores) across time (x-axis; from 0 to 1500 ms poststimulus) and frequency (y-axis; from 4 to 8 Hz) is plotted for each electrode for WC (left), WO (middle), and Miss (right) conditions. In Fig. 1d, TF significance maps show P values for TF pixels reaching a $P < 0.05$ threshold for the comparisons WC > Miss (left), WO > Miss (middle), and WC > WO (right). A theta increase is initially seen in all three conditions;
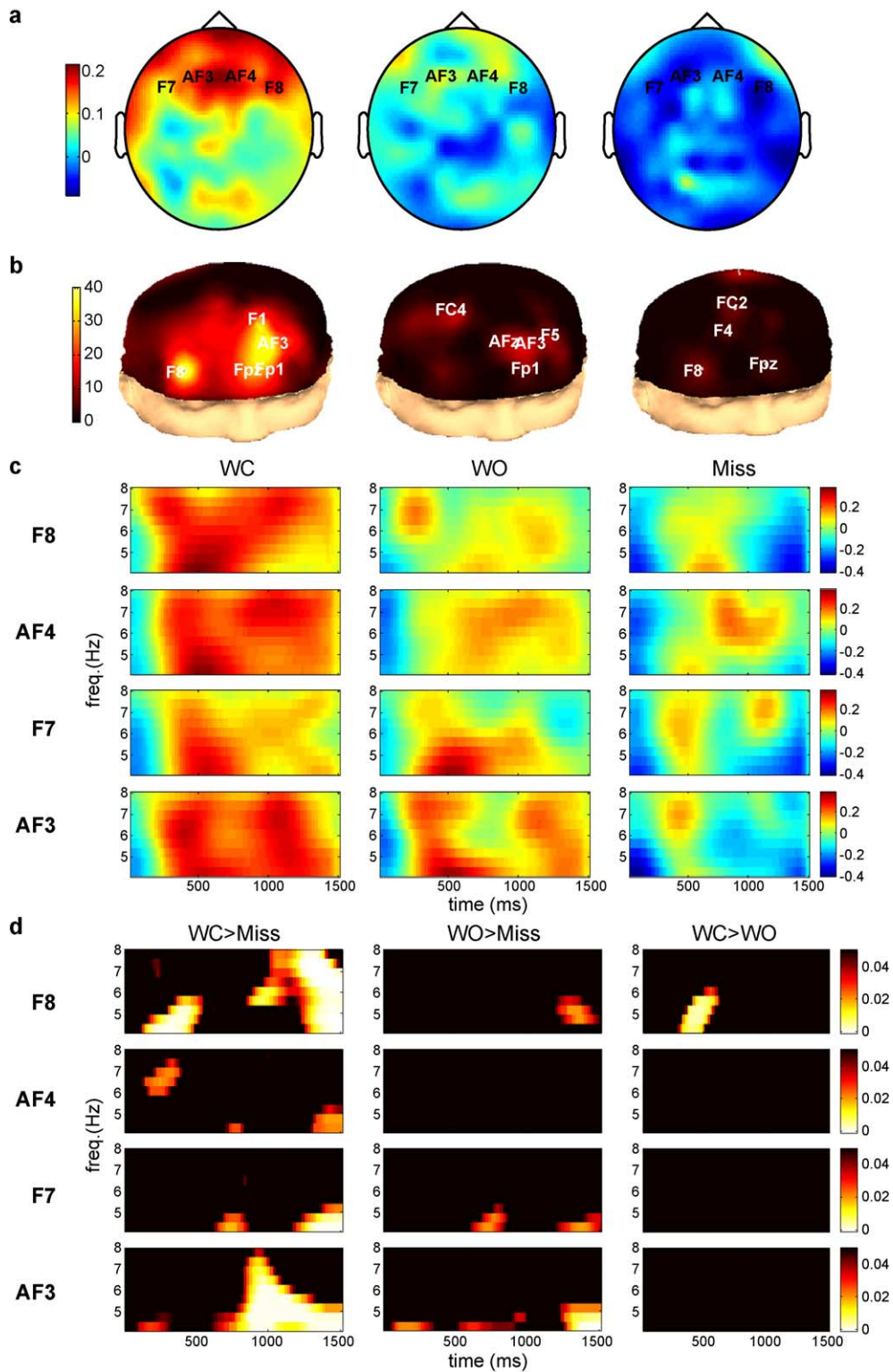
Fig. 1. Local frontal theta activity predicts subsequent memory. (a) Mean theta power across the epoch for WC (left), WO (middle), and Miss trials (right). (b) Brain regions showing significant differences in theta power for comparisons WC > Miss (left), WO > Miss (middle), and WC > WO (right). Scale refers to percentage of pixels across TF space reaching $P < 0.05$ significance. (c) Mean time–frequency profile of theta-band activity for four representative frontal electrodes. Values are mean z scores across subjects. (d) Regions of TF space showing significant differences for the three comparisons. Scale refers to P values; only P values <0.05 are shown.

however, this response is more sustained in WC (and to a lesser extent, WO) trials. Thus, significant differences relating to successful encoding mainly occur late (>1000 ms) in the epoch at the frontal electrodes (Fig. 1d, note left and middle panels), and span the theta band (4–8 Hz). There was also a tendency for right frontal electrodes (F8, F6, AF4, FP2) to show significant differences during earlier portions of the epoch (Fig. 1d, top left). At right frontal electrodes F8, significant differences between WC and WO trials were also observed at approximately 400 ms (Fig. 1d, top right panel). Effects, notably for the comparison WC > Miss, were very robust (many pixels reached a significance threshold of $P < 0.001$,

corrected for multiple comparisons across TF space; maximally, 40% of all pixels across time–frequency space achieved significance at corrected $P < 0.05$).

Local theta activity: ICA analyses

The ICA component accounting for the greatest percentage of variance (20.1%; eigenvalue = 21.6) loaded principally on frontal electrodes (Fig. 2a, left panel). The scale on the scalpmaps in Fig. 2a refers to the ICA weight of each electrode for that particular component, interpolated across the scalp. As might be expected from the electrode-wise analyses, the TF profile of the activations
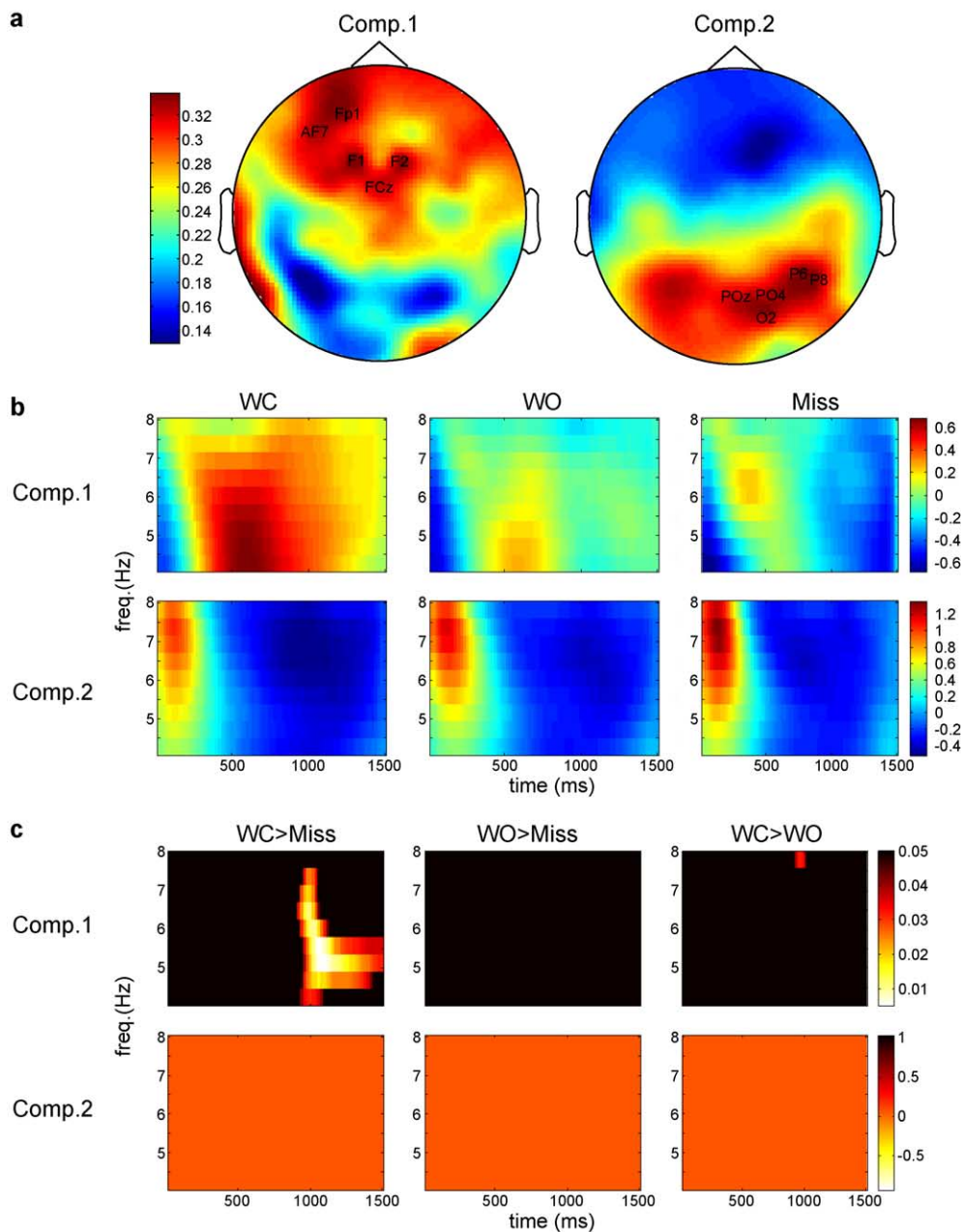

Fig. 2. ICA analysis of local theta activity. (a) Scalp distribution of ICA components 1 (left) and 2 (right). (b) Mean component activations (weights* input data) for each component (top, component 1; bottom, component 2) for each condition (left, WC; middle, WO; right, miss). (c) Areas of TF space showing significance for comparisons WC > Miss (left), WO > Miss (middle), and WC > WO (right). No significant differences between conditions are observed for the second component.

showed a robust and sustained poststimulus theta response (Fig. 2b, top) that was greater for WC trials than for Misses, particular in the latter portion of the epoch and centered around 5 Hz (Fig. 2c, top left). There was also a very small region in the upper theta band that showed significant differences between WC and WO trials ($P < 0.04$, Fig. 2c, top right). However, unlike the electrode-wise analysis described above, no differences were observed between WO trials and Misses (Fig. 2c, top middle). In addition, the ICA did not further dissociate the left and right hemisphere asymmetry suggested by the electrode-wise analysis of successful word or word + color encoding, respectively.

Although the subsequent three ICA components accounted for at least 22.1% of the variance or more (sum of eignenvalues = 11.2; range = 6.4–2.0), these did not discriminate between conditions. For example, the second component (Fig. 2a, right panel; Fig. 2b,

bottom panel), which loaded principally on posterior electrodes and accounted for 11.3% of the variance (eigenvalue = 6.4), showed a theta response early (approximately 200 ms) in the poststimulus epoch that did not differ between the three conditions (Fig. 2c, bottom panel).

Long-range theta activity: pairing-wise analyses

Across the entire scalp, electrode pairings for which significant differences were observed between conditions are plotted in Fig. 3a. A significant pairing was considered to be any pair for which at least 1 TF pixel was significant at the more conservative threshold of $P < 0.01$ (corrected for multiple comparisons across TF space) for a given contrast (i.e., WC > Miss). As illustrated in Fig. 3a, significant electrode pairings were observed for all three compar-
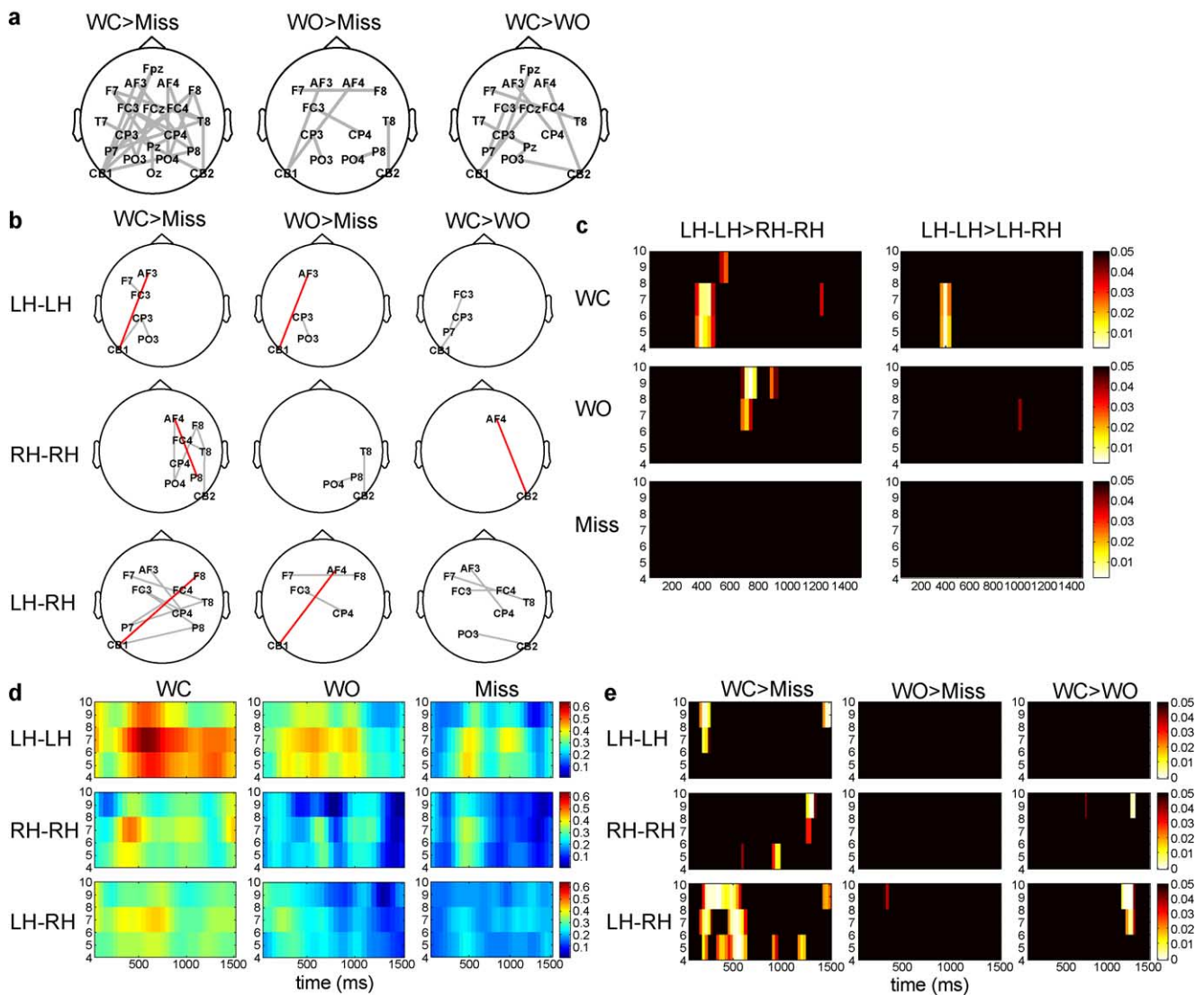

Fig. 3. Long-range theta coherence predicts subsequent memory. (a) All electrode pairings for which significant ($P < 0.01$) coherence was observed at least 1 TF pixel, for the comparisons WC > Miss (left), WO > Miss (middle), and WC > WO (right). (b) Electrode pairings that exhibit significant coherence within the left hemisphere (top row), within the right hemisphere (middle row), and between the two hemispheres (bottom row) for the three comparisons. Frontoposterior pairings are marked in red. (c) Hemispheric contributions to coherence. For each condition, significant differences are shown for comparisons LH–LH > RH–RH (left) and LH–LH > LH–RH (right). (d) Mean TF profile of coherence for all LH–LH (top), RH–RH (middle), and LH–RH pairings (bottom), for each of the three conditions. (e) Significance maps for comparisons WC > Miss (left), WO > Miss (middle), and WC > WO (right) for mean intra- and interhemispheric frontoposterior coherence.

isons, although a numerically greater quantity of significant pairings was observed for WC > Miss ($n = 27$) and WC > WO ($n = 11$) than for WO > Miss ($n = 7$). No electrode pairings were significant for the comparisons Miss > WC or Miss > WO.

In accordance with our prediction that frontoposterior activity would predict successful encoding, we focused subsequent analyses on pairings between anterior frontal (F7, F8, AF3, AF4, Fpz) and inferior posterior (Cb1, Cb2, Oz, P7, P8) electrodes. Notably, these electrodes correspond closely to the cortical regions activated in Ranganath et al. (2004) in association with word and word + color encoding. For display purposes, coherent interactions between these frontoposterior electrodes are highlighted in red. In addition, we plotted significant LH–LH, RH–RH, and LH–RH pairings for each comparison on separate figures in order to determine how left intrahemispheric (LH–LH), right intrahemispheric (RH–RH), and interhemispheric (LH–RH) coherence differed as a function of trial type at these pairings (Fig. 3b).

Visual inspection of Fig. 3b (top) shows that significant pairings are observed for the comparison WC > Miss both inter- and intrahemispherically. Intrahemispherically, a dissociation is observed whereby LH–LH frontoposterior coherence (CB1–AF3) is significant for both WC > Miss and WO > Miss, whereas RH–RH frontoposterior coherence (CB2–AF4) is significantly greater for comparisons WC > Miss and WC > WO (Fig. 3b). This suggests that left intrahemispheric coherence contributes to successful word encoding in either the WC or WO conditions, whereas right intrahemispheric coherence may be preferentially involved during successful binding of word + color.

Examination of the time–frequency course of averaged LH–LH, RH–RH, and LH–RH frontoposterior electrode pairings revealed prominent theta coherence at approximately 500 ms on WC trials for both intra- and interhemispheric electrode pairings (Fig. 3d, left). This response was most prominent not only in the upper theta band (6–8 Hz), but also extended into the lower theta (4–6 Hz) and lower alpha (8- to 10-Hz frequencies). A response with a similar TF profile was observed for WO trials, but visual inspection suggested that it was confined to the left hemisphere (Fig. 3d, top middle). Values for Fig. 3d are "corrected" coherence (i.e., [z transformed "intact" coherence] - [z transformed "shuffled" coherence]).

In order to determine whether this effect of hemisphere was statistically robust, we performed a 3 [condition] * 3 [hemisphere] ANOVA across TF space for these frontoposterior pairings. Significant effects of condition and hemisphere were observed. However, the omnibus interaction term did not reach $P < 0.05$ at any TF pixels (not shown). The effect of condition for LH–LH, RH–RH, and LH–RH coherence is displayed in Fig. 3e. Notably, a WC > WO profile of statistical reliability at >1000 ms is only observed for frontoposterior coherence within the right hemisphere, and intrahemispherically, suggesting that item-context binding is preferentially mediated by networking within right-hemisphere structures.

In Fig. 3c, we explored the main effect of hemisphere with planned comparisons, comparing hemispheres (LH–LH, RH–RH, and LH–RH) for each trial type. Of the six possible comparisons, only LH–LH > RH–RH and LH–LH > LH–RH showed significance. In Fig. 3c, it can be seen that overall, greater
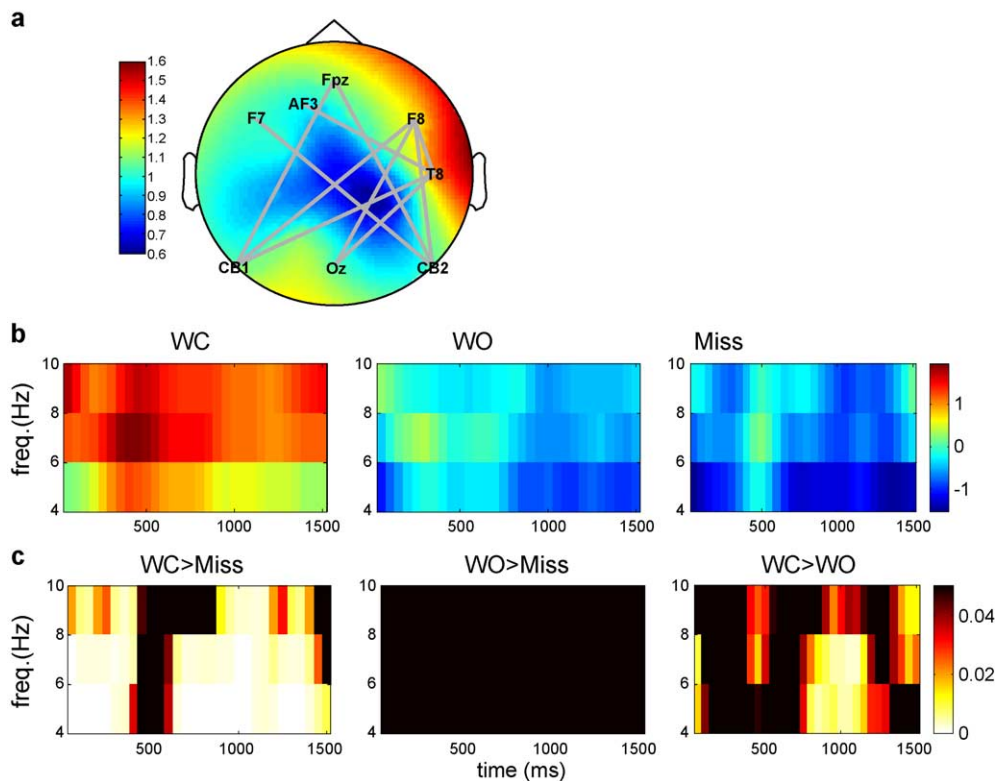

Fig. 4. ICA analysis of long-range theta coherence. (a) The component showing significant differences between conditions. The 10 electrode pairings with the highest weights are plotted on a background of total ICA weights for each electrode (summed across pairings). (b) Mean corrected coherence across TF space for the component. Conditions are WC (left), WO (middle), and Miss (right). (c) Areas of TF space that show greater coherence for the comparisons WC > Miss (left), WO > Miss (middle), and WC > WO (right).

frontoposterior theta coherence was observed at approximately 500 within the left hemisphere for correct (WC and WO) trials, relative to right-hemisphere or intrahemispheric coherence.

Long-range theta activity: ICA analyses

In order to reduce the 190 electrode pairings to a manageable number of components, we employed spatial ICA with four-component PCA preprocessing. Activation scores (reflecting weights * input data) and component weights at each electrode paring were visualized for the four components accounting for the greatest percentage (total 15.5%; sum of eigenvalues 1 to 4 = 4.7) of the variance. The component accounting for the greatest percentage of the variance (6.0%; eigenvalue = 1.8) exhibited significant differences between conditions. To simplify the visual display, we plotted the 10 electrodes with the highest weights (grey lines) on top of the sum of component weights for each electrode interpolated across the scalp (Fig. 4a). All 10 of the electrode pairings that loaded most highly on component 1 showed phase locking within a triangular network encompassing left frontal, right frontotemporal, and posterior electrode sites: Oz- F8, Oz- T8, F7-CB1, F8-CB1, T8-CB1, Fpz-CB2, Fpz-CB1, F8-CB2, AF3-T8 T8-F8 (Fig. 4a).

Fig. 4b shows mean 'corrected' coherence across TF space. Coherence began at stimulus onset in the upper theta band, peaking at approximately 500 ms poststimulus. Fig. 4c details TF regions achieving $P < 0.05$ significance for between-condition comparisons. The first component showed significant differences in coherence for the comparisons WC > Miss and WC > WO, but not for WO > Miss, suggesting that frontoposterior coherence was specifically associated with WC trials (Fig. 4c). Significant differences between WC and Miss trials were observed during the early (<400 ms) and late (>600 ms) phases of the epoch. Significant differences (corrected for multiple comparisons across TF space and components) between WC and WO trials were observed at 400 and >600 ms (maximally at approximately 1000 ms) poststimulus (Fig. 4c). This pattern of results suggests, as for local theta data, that while coherence at the approximately 500 ms peak did not differ significantly between comparisons, sustained coherence (>500 ms) was a strong predictor of subsequent memory for the word-color association.

Discussion

Summary

The present study reports patterns of local and long-range theta-band activity during encoding that predict subsequent memory for an item with or without its associated context. We used planned comparisons to distinguish between neural activity predicting successful encoding of a word and its associated font color (item + context encoding; indicated by significance for comparisons WC > Miss and WC > WO) and activity predicting subsequent later word recognition only (item encoding; WC > Miss and WO > Miss). Item encoding was associated with sustained local theta activity over left frontal regions and increases in long-range coherence within the left hemisphere, notably between left inferior posterior and anterior frontal regions. On trials for which item + context encoding occurred, we additionally observed early (approximately 400 ms) increases in theta power mainly over right anterior frontal

regions and increased late (>800 ms) frontoposterior coherence that additionally engaged the right hemisphere. ICA analyses confirmed the importance of sustained bilateral frontoposterior coherence in the encoding of item and context.

Item encoding

Consistent with previous reports (Klimesch et al., 1996; Sederberg et al., 2003), increases in local synchrony over frontal areas were observed during the encoding of words that were later correctly identified as 'old' on an old/new recognition test (Figs. 1 and 2). At left frontal electrodes, we observed that it is less the strength of the initial (approximately 300 ms) theta burst, but more the extent to which the theta response is sustained during the encoding epoch, which predicted subsequent word recognition. This was indicated by the finding that significant differences were observed late (>1000 ms) in the epoch for the comparisons WC > Miss and WO > Miss. A sustained left frontal theta response predicting later memory for a word may reflect rehearsal or elaboration in verbal working memory. Consistent with this hypothesis, an association has been reported between theta activity and working memory (Bastiaansen and Hagoort, 2003; Gevins and Smith, 2000; Raghavachari et al., 2001; Sarnthein et al., 1998; Sauseng et al., 2004; Tesche and Karhu, 2000), and other studies have also noted that activation in brain areas involved in phonological rehearsal predict subsequent memory (Davachi et al., 2001; Nyberg et al., 1996). ICA results on the local theta data confirmed the finding that frontal theta activity accounted for the greatest percentage of the variance between conditions and was statistically reliable ($P < 0.001$) at the more conservative correction threshold (Fig. 2).

Significantly greater coherence between left hemisphere electrodes CB1 and AF3 was observed for WC and WO than Miss trials (Fig. 3b). No frontoposterior pairings within the left hemisphere for the comparison WC > WO reached statistical threshold, suggesting an effect specific to item encoding. Successful encoding of the semantic attributes of a word stimulus is likely to demand the sharing of information between ventral stream association areas, perhaps involving the visual word form area (Cohen et al., 2002) and left frontal regions thought to play a role in semantic retrieval (Thompson-Schill, 2003). One possibility is that during item encoding, neurons in the left frontal structures begin to exhibit rhythmic theta activity, which, when sufficiently sustained, recruits a phase-locked response from neurons in the left posterior association areas. Such activity may form a correlate of neural integration during item encoding.

Item + context encoding

Right frontal theta activity close to 500 ms was significantly greater for WC than Miss or WO trials. This suggests that local increases in theta power over right frontal regions were more specific to trials on which the word + color association was successfully encoded. This observation is not without precedent. A recent study has reported that right frontal theta activity close to 500 ms poststimulus predicts later word recall (Sederberg et al., 2003). In addition, an fMRI study using a highly similar task noted that activation in the right inferior frontal gyrus (BA 44; roughly corresponding to the placement of our electrode F8) predicted successful encoding of a word and its font color (Ranganath et al., 2004). The time course of local synchrony involving right anterior

regions also shows good correspondence with the findings of an ERP study dissociating encoding trials leading to later R and K responses, in which R > K showed a right anterior topography with differences at 400–600 ms poststimulus (Duarte et al., 2004).

Coherence analyses suggested that item + context encoding was associated with phase locking in the theta band between frontal and posterior electrode sites bilaterally. A clear peak in mean coherence in the upper portion of the theta band (6–8 Hz) is visible at approximately 500 ms in the mean coherence plots for WC trials (Fig. 3d). Pairing-wise analyses revealed greater frontoposterior coherence within the right hemisphere for WC than for WO or Miss trials. ICA analysis confirmed the bilateral nature of the coherence associated with item + context encoding. The component that accounted for the greatest percentage of the variance strongly predicted successful encoding of item + context, and loaded principally on coherent interactions between left frontal electrodes, such as F7, FC3 Fpz, right frontotemporal electrodes F8 and T8, and bilateral occipital/infero-temporal electrodes Oz, CB1, and CB2. In addition, both pairing-wise and ICA analyses suggested that differences in theta coherence associated with word + color encoding were maximal at >800 ms, suggesting that, as for local theta data, it is the presence of sustained frontoposterior phase locking in the theta band that predicts item-context binding.

Previous studies have highlighted the role that frontoposterior coherence may play in learning. Coherence between frontal and posterior areas has been implicated in working memory (Sarnthein et al., 1998), and coherence between frontal and posterior regions has been shown to occur during word encoding associated with successful recall and recognition (Sauseng et al., 2004; Weiss and Rappelsberger, 2000). In addition, an earlier ERP study reported a sustained right positivity during encoding that occurred concurrently at right frontal and posterior electrode sites over the later portion of the encoding epoch, perhaps reflecting neural integration between these areas, which predicted later 'R' responses for words (Mangels et al., 2001). Here, we confirm the importance of frontoposterior coherence in encoding, and present evidence firstly, that there is a strong peak in coherence at 500 ms poststimulus, and secondly, that it is the degree to which this coherence is sustained that predicts associative encoding (Figs. 3d–e and 4b–c). Contemporary models of working memory have proposed that during short-term storage, posterior perceptual and association areas are maintained tonically active through connections with the prefrontal cortex (Cowan, 1995). Frontal lobe regions found to be active in neuroimaging studies of working memory may thus act as an attentional 'pointer', defining which posterior representations to hold online or semantically elaborate. Our data suggest that synchronous activity in the theta band plays an important role in this process, mediating crosstalk between anterior and posterior regions during maintenance and elaboration in working memory, and increasing the likelihood of encoding into a long-term memory. This process may occur via collaboration with medial temporal lobe structures, although this remains to be determined.

Asymmetric contributions to encoding of item and context

We observed an interesting dissociation in the contributions of the left and right hemispheres to encoding of item and context. Coherence between left anterior and left posterior sites was associated with encoding of the word, irrespective of whether the font color was encoded, but greater coherence involving the right hemisphere was additionally observed when subjects later retrieved both word and color. Accordingly, recent fMRI and ERP studies have found left-hemisphere activity to be more predictive of later word-only recognition (Ranganath et al., 2004) or item familiarity (Duarte et al., 2004), whereas right-hemisphere activity was more specific to encoding leading to later recollection (Duarte et al., 2004). Frontoposterior coherence during spatial and verbal working memory maintenance has also been shown to be lateralized in a similar fashion (Sarnthein et al., 1998). These data are consistent with a theoretical perspective that the left brain is involved in lexical–semantic memory processing, whereas the right brain may process the sensory detail that accompanies episodic memory (Gazzaniga, 2000), a theory that dates back to Paivio (1971). It could thus be that episodic encoding requires integration of semantic (left hemisphere) and contextual (right hemisphere) attributes of a stimulus, such that a rich, detailed episodic memory trace is laid down in long-term memory.

Our data do not suggest that contributions to episodic encoding are equally shared between the left and right hemispheres, however. Indeed, we observed a main effect of hemisphere in frontoposterior coherence, with greater theta coherence within the left hemisphere than within the right or between the two hemispheres (at approximately 500 ms), when encoding was successful (Fig. 4e). This pattern is consistent with an extensive literature supporting the Hemispheric Encoding and Retrieval Asymmetry (HERA) model that episodic encoding may be differentially left lateralized (Habib et al., 2003).

Nonetheless, there are two reasons why we believe that the effects of lateralization described here must be treated with caution. Firstly, in our study, ICA analyses failed to dissociate left from right hemisphere contributions to item and context encoding. This suggests that overall, there was a strong correlation in the spatiotemporal pattern of encoding-related activity between the two hemispheres. Secondly, our effect is largely descriptive, with numerically greater numbers of significant electrode pairings observed on the right than left in association with item + context encoding. Although many neuroimaging papers draw inferences from purely descriptive patterns of data ('more significance on the left than right'), these effects may vary as a function of an arbitrarily imposed statistical threshold, rather than truly reflecting the extent of an effect (Jernigan et al., 2003). Further, when we subjected the lateralization effect to direct statistical analysis, we failed to find a significant interaction between condition and hemisphere for the coherence data. Thus, we believe that these lateralization effects must be considered 'exploratory' until confirmed through replication.

Methodological considerations

An additional goal of this report was to present a novel approach to the visualization and statistical testing of time–frequency and coherence EEG data. The approach was motivated by the need to provide a correction for multiple comparisons that reduces both type-1 and type-2 errors. Under the framework of the analyses conducted here, an exploration of the spatiotemporal signature of a neural effect (difference between conditions on a given task) is conducted by comparing

time–frequency pixels across the brain using random permutation testing and correcting for multiple-comparisons across time–frequency space but not across spatial observations (electrodes or electrode pairings). In a second stage, ICA is used to reduce the data to spatially correlated components, and significance testing is repeated, correcting for multiple comparisons across components, thus providing a more conservative statistical threshold. The logic of this approach is that although each spatial sampling point (electrode or electrode pairing) may not be statistically independent, components derived from ICA are likely to be so. Thus, by correcting for multiple comparisons across all ICA components, we are correcting across statistically independent spatial observations across the scalp.

We accept that there are limitations to this approach. Firstly, ICA may not perfectly separate statistically independent contributions to between-condition variance. As mentioned above, ICA analysis confirmed that local theta contributions to encoding were bilateral across frontal regions, but it did not dissociate left and right frontal contributions to item and context encoding, despite the fact that this difference was visible in the electrode-wise analyses. Secondly, one of the problems with our ICA approach to data reduction is how to determine the optimal number of PCA preprocessing components. Our approach was to explore the data using different numbers of PCA preprocessing components using visual inspection of the results to determine how many should be reported. It could be argued that this method is somewhat arbitrary. Given that during ICA analyses, we corrected for multiple comparisons across a number of components equivalent to the number of preprocessing components selected, the absolute number of observations also differed as a function of this variable. However, in simulation analyses, we have found that the spatial/TF profile of an effect and the level of significance tend to remain constant regardless of the number of components. For example, with many solutions, the weights and activations of two components will exhibit a strong overlap, suggesting that ICA is dividing a single neural effect into two components. Under these conditions, statistically significant pixels may be distributed across the two components, but the total number of significant pixels remains constant. Variance explained by our coherence components, while smaller than that often observed in PCA-based data reduction techniques, was comparable to that often observed in ICA analysis (Makeig et al., 2004).

However, for both local and long-range theta activity, ICA analysis confirmed that the main effects observed in the e/p-wise analyses were those extracted by ICA as components accounting for the greatest percentage of the between-condition variance. Further, significance testing with spatial (as well as TF) correction for multiple comparisons confirmed that these results were statistically reliable.

Finally, it is unlikely that theta-band EEG activity is the only mechanism by which information is shared between neural systems during encoding. Other studies have recently shown that increases in local gamma-band (25–55 Hz) activity in the neocortex (Babiloni et al., 2004; Sederberg et al., 2003) and long-range coherence between the hippocampus and perirhinal cortex (Fell et al., 2003) are also associated with encoding. Further, it has been argued that first-order coherence may not be the best measure of functional coupling between neural assemblies (Friston, 1997). Therefore, it would be of interest for future studies to examine whether local and long-range interactions between theta-band and gamma-band EEG activity contribute to associative or nonassociative encoding.

References

Babiloni, C., Babiloni, F., Carducci, F., Cappa, S., Cincotti, F., Del Percio, C., Miniussi, C., Moretti, D.V., Pasqualetti, P., Rossi, S., et al., 2004. Human cortical EEG rhythms during long-term episodic memory task. A high-resolution EEG study of the HERA model. NeuroImage 21, 1576–1584.

Bastiaansen, M., Hagoort, P., 2003. Event-induced theta responses as a window on the dynamics of memory. Cortex 39, 967–992.

Bell, A.J., Sejnowski, T.J., 1995. An information-maximization approach to blind separation and blind deconvolution. Neural Comput. 7, 1129–1159.

Berg, P., Scherg, M., 1994. A multiple source approach to the correction of eye artifacts. Electroencephalogr. Clin. Neurophysiol. 90, 229–241.

Burgess, A.P., Gruzelier, J., 1999. Methodological Advances in the Analysis Of Event-Related Desynchronisation Data: Reliability and Robust Analysis.

Buzsaki, G., 1996. The hippocampo-neocortical dialogue. Cereb. Cortex 6, 81–92.

Cansino, S., Maquet, P., Dolan, R.J., Rugg, M.D., 2002. Brain activity underlying encoding and retrieval of source memory. Cereb. Cortex 12, 1048–1056.

Cohen, L., Lehericy, S., Chochon, F., Lemer, C., Rivaud, S., Dehaene, S., 2002. Language-specific tuning of visual cortex? Functional properties of the visual word form area. Brain 125, 1054–1069.

Cowan, N., 1995. Attention and Memory: An Integrated Framework. Oxford Univ. Press.

Crick, F., Koch, C., 1990. Some reflections on visual awareness. Cold Spring Harbor Symp. Quant. Biol. 55, 953–962.

Davachi, L., Maril, A., Wagner, A.D., 2001. When keeping in mind supports later bringing to mind: neural markers of phonological rehearsal predict subsequent remembering. J. Cogn. Neurosci. 13, 1059–1070.

Davachi, L., Mitchell, J.P., Wagner, A.D., 2003. Multiple routes to memory: distinct medial temporal lobe processes build item and source memories. Proc. Natl. Acad. Sci. U. S. A. 100, 2157–2162.

Delorme, A., Makeig, S., 2004. EEGLAB: an open source toolbox for analysis of single-trial EEG dynamics including independent component analysis. J. Neurosci. Methods 134, 9–21.

Duarte, A., Ranganath, C., Winward, L., Hayward, D., Knight, R.T., 2004. Dissociable neural correlates for familiarity and recollection during the encoding and retrieval of pictures. Brain Res., Cogn. Brain Res. 18, 255–272.

Engel, A.K., Fries, P., Singer, W., 2001. Dynamic predictions: oscillations and synchrony in top-down processing. Nat. Rev., Neurosci. 2, 704–716.

Fell, J., Klaver, P., Elfadil, H., Schaller, C., Elger, C.E., Fernandez, G., 2003. Rhinal–hippocampal theta coherence during declarative memory formation: interaction with gamma synchronization? Eur. J. Neurosci. 17, 1082–1088.

Friston, K.J., 1997. Another neural code? NeuroImage 5, 213–220.

Gazzaniga, M.S., 2000. Cerebral specialization and interhemispheric communication: does the corpus callosum enable the human condition? Brain 123 (Pt 7), 1293–1326.

Gevins, A., Smith, M.E., 2000. Neurophysiological measures of working memory and individual differences in cognitive ability and cognitive style. Cereb. Cortex 10, 829–839.

Givens, B.S., Olton, D.S., 1990. Cholinergic and GABAergic modulation of medial septal area: effect on working memory. Behav. Neurosci. 104, 849–855.

Habib, R., Nyberg, L., Tulving, E., 2003. Hemispheric asymmetries of memory: the HERA model revisited. Trends Cogn. Sci. 7, 241–245.

Huerta, P.T., Lisman, J.E., 1993. Heightened synaptic plasticity of hippocampal CA1 neurons during a cholinergically induced rhythmic state. Nature 364, 723–725.

Janowsky, J.S., Shimamura, A.P., Squire, L.R., 1989. Source memory impairment in patients with frontal lobe lesions. Neuropsychologia 27, 1043–1056.

Jensen, O., Lisman, J.E., 1996. Theta/gamma networks with slow NMDA channels learn sequences and encode episodic memory: role of NMDA channels in recall. Learn Mem. 3, 264–278.

Jernigan, T.L., Gamst, A.C., Fennema-Notestine, C., Ostergaard, A.L., 2003. More "mapping" in brain mapping: statistical comparison of effects. Hum. Brain Mapp. 19, 90–95.

Kahana, M.J., Sekuler, R., Caplan, J.B., Kirschen, M., Madsen, J.R., 1999. Human theta oscillations exhibit task dependence during virtual maze navigation. Nature 399, 781–784.

Klimesch, W., Doppelmayr, M., Russegger, H., Pachinger, T., 1996. Theta band power in the human scalp EEG and the encoding of new information. NeuroReport 7, 1235–1240.

Lachaux, J.P., Lutz, A., Rudrauf, D., Cosmelli, D., Le Van Quyen, M., Martinerie, J., Varela, F., 2002. Estimating the time-course of coherence between single-trial brain signals: an introduction to wavelet coherence. Neurophysiol. Clin. 32, 157–174.

Lee, T.W., Girolami, M., Sejnowski, T.J., 1999. Independent component analysis using an extended infomax algorithm for mixed subgaussian and supergaussian sources. Neural Comput. 11, 417–441.

Makeig, S., Debener, S., Onton, J., Delorme, A., 2004. Mining event-related brain dynamics. Trends Cogn. Sci. 8, 204–210.

Mangels, J.A., Picton, T.W., Craik, F.I., 2001. Attention and successful episodic encoding: an event-related potential study. Brain Res., Cogn. Brain Res. 11, 77–95.

McKeown, M.J., Hansen, L.K., Sejnowsk, T.J., 2003. Independent component analysis of functional MRI: what is signal and what is noise? Curr. Opin. Neurobiol. 13, 620–629.

Nunez, P.L., Srinivasan, R., Westdorp, A.F., Wijesinghe, R.S., Tucker, D.M., Silberstein, R.B., Cadusch, P.J., 1997. EEG coherency. I: statistics, reference electrode, volume conduction, laplacians, cortical imaging, and interpretation at multiple scales. Electroencephalogr. Clin. Neurophysiol. 103, 499–515.

Nyberg, L., McIntosh, A.R., Cabeza, R., Habib, R., Houle, S., Tulving, E., 1996. General and specific brain regions involved in encoding and retrieval of events: what, where, and when. Proc. Natl. Acad. Sci. U. S. A. 93, 11280–11285.

Otten, L.J., Henson, R.N., Rugg, M.D., 2002. State-related and item-related neural correlates of successful memory encoding. Nat. Neurosci. 5, 1339–1344.

Paivio, A., 1971. Imagery and verbal processes. Holt Rhinehart & Wilson, New York.

Raghavachari, S., Kahana, M.J., Rizzuto, D.S., Caplan, J.B., Kirschen, M.P., Bourgeois, B., Madsen, J.R., Lisman, J.E., 2001. Gating of human theta oscillations by a working memory task. J. Neurosci. 21, 3175–3183.

Ranganath, C., Yonelinas, A.P., Cohen, M.X., Dy, C.J., Tom, S.M., D'Esposito, M., 2004. Dissociable correlates of recollection and familiarity within the medial temporal lobes. Neuropsychologia 42, 2–13.

Rodriguez, E., George, N., Lachaux, J.P., Martinerie, J., Renault, B., Varela, F.J., 1999. Perception's shadow: long-distance synchronization of human brain activity. Nature 397, 430–433.

Roelfsema, P.R., Engel, A.K., Konig, P., Singer, W., 1997. Visuomotor integration is associated with zero time-lag synchronization among cortical areas. Nature 385, 157–161.

Sarnthein, J., Petsche, H., Rappelsberger, P., Shaw, G.L., von Stein, A., 1998. Synchronization between prefrontal and posterior association cortex during human working memory. Proc. Natl. Acad. Sci. U. S. A. 95, 7092–7096.

Sauseng, P., Klimesch, W., Doppelmayr, M., Hanslmayr, S., Schabus, M., Gruber, W.R., 2004. Theta coupling in the human electroencephalogram during a working memory task. Neurosci. Lett. 354, 123–126.

Scoville, W.B., Milner, B., 1957. Loss of recent memory after bilateral hippocampal lesions. J. Neurochem. 20, 11–21.

Sederberg, P.B., Kahana, M.J., Howard, M.W., Donner, E.J., Madsen, J.R., 2003. Theta and gamma oscillations during encoding predict subsequent recall. J. Neurosci. 23, 10809–10814.

Singer, W., Gray, C.M., 1995. Visual feature integration and the temporal correlation hypothesis. Annu. Rev. Neurosci. 18, 555–586.

Tallon-Baudry, C., Bertrand, O., 1999. Oscillatory gamma activity in humans and its role in object representation. Trends Cogn. Sci. 3, 151–162.

Tesche, C.D., Karhu, J., 2000. Theta oscillations index human hippocampal activation during a working memory task. Proc. Natl. Acad. Sci. U. S. A. 97, 919–924.

Thompson-Schill, S.L., 2003. Neuroimaging studies of semantic memory: inferring "how" from "where". Neuropsychologia 41, 280–292.

Tononi, G., Edelman, G.M., 1998. Consciousness and complexity. Science 282, 1846–1851.

Torrence, C., Campo, G.P., 1998. A practical guide to wavelet analysis. Am. Meteorol. Soc. 79.

Varela, F.J., 1995. Resonant cell assemblies: a new approach to cognitive functions and neuronal synchrony. Biol. Res. 28, 81–95.

Wagner, A.D., Schacter, D.L., Rotte, M., Koutstaal, W., Maril, A., Dale, A.M., Rosen, B.R., Buckner, R.L., 1998. Building memories: remembering and forgetting of verbal experiences as predicted by brain activity. Science 281, 1188–1191.

Weiss, S., Rappelsberger, P., 2000. Long-range EEG synchronization during word encoding correlates with successful memory performance. Brain Res., Cogn. Brain Res. 9, 299–312.